J. Fluid Mech. (1972), *vol.* 51, *part* 2, *pp.* 221–231
Printed in Great Britain

Cavity flows driven by buoyancy and shear

By K. TORRANCE, R. DAVIS, K. EIKE, P. GILL, D. GUTMAN, A. HSUI, S. LYONS AND H. ZIEN
Department of Thermal Engineering, Cornell University, Ithaca, New York

(Received 2 April 1971)

Fluid motion driven by the combined effects of a moving wall and natura convection is examined for rectangular cavities with height/width ratios of $\frac{1}{2}$, 1 and 2. The Reynolds number and Prandtl number are held fixed at $Re = 100$ and $Pr = 1$; the Grashof number is varied over the range of values $Gr = 0, \pm 10^4, \pm 10^6$. Flow and temperature fields obtained from numerical solutions of the Navier–Stokes equations reveal a marked influence of buoyancy for the larger aspect ratios when $Gr = \pm 10^4$ and the dominance of buoyancy for all aspect ratios when $Gr = \pm 10^6$. Results are compared with earlier work where possible and some observations are offered on the convergence of the numerical solutions.

1. Introduction

This study examines fluid motion generated in a rectangular cavity by a moving upper wall. In contrast to previous work, the moving wall is maintained at a temperature different from the remaining walls of the cavity and natural convection is permitted. The resulting fluid motion is driven by the combined effects of wall shear and buoyancy. Such a cavity simulates a lubricating groove between sliding plates or, approximately, the separated flow in a surface cavity with an external stream flowing over it.

Cavity flows generated by a moving wall in the absence of buoyancy effects have been studied for a wide range of Reynolds numbers. Experimental results are reported by Pan & Acrivos (1967), Weiss & Florsheim (1965) and Mills (1965) for cavities of several aspect ratios (height/width) and analytical results are available for Reynolds numbers which are either very low (Pan & Acrivos 1967; Weiss & Florsheim 1965) or very high (Batchelor 1956; Squire 1956). For flows in which both viscous and inertia terms are important (intermediate Reynolds numbers) numerical solutions of the Navier–Stokes equations have been required. Recent work is summarized by Donovan (1970) and Greenspan (1969); earlier work has been presented by Mills (1965), Simuni (1964) and Kawaguti (1961). The accuracy of numerical solutions is discussed by Gosman *et al.* (1969) and Burggraf (1966) for the case of a square cavity. Natural convection flows in a rectangular cavity with stationary, non-isothermal walls are of interest for heat-transfer calculations; a summary of pertinent work is presented by Newell & Schmidt (1970).

The present study had its origins in a graduate course on numerical fluid dynamics in which the cavity problem, with and without buoyancy, constituted

the final examination. Surprisingly, results revealed that flows driven by the combined effects of buoyancy and shear were quite different from those driven by the separate effects. The study was consequently extended to a sequence of finer computing grids and to a range of buoyancy parameters. Each student wrote his own computing algorithm and applied it to a number of cases for which results were desired. Results were overlapping. The purpose of presenting the work here is threefold: first, to illustrate flows driven by both buoyancy and shear; second, to present some observations on convergence of the numerical method; third, to demonstrate that numerical solutions of complex flow problems may be obtained with a modest effort (a one-semester effort being considered modest).

2. Problem formulation

Consider a two-dimensional cavity of width d and height h in which the upper wall moves across the cavity from left to right at a constant speed U. Erect an x, y co-ordinate system at the lower left corner of the cavity, with y vertical. The upper wall is at temperature T_1 and the remaining walls are at temperature T_0. Using d, U and $(T_1 - T_0)$ as reference length, velocity and temperature, the governing equations in a vorticity-stream function formulation become:

$$\frac{\partial T}{\partial t} + \nabla . (\mathbf{u}T) = \frac{1}{Re\,Pr} \nabla^2 T, \tag{1}$$

$$\frac{\partial \omega}{\partial t} + \nabla . (\mathbf{u}\omega) = \frac{Gr}{Re^2} \frac{\partial T}{\partial x} + \frac{1}{Re} \nabla^2 \omega, \tag{2}$$

$$\omega = -\nabla^2 \psi, \tag{3}$$

$$u_x = \frac{\partial \psi}{\partial y}, \quad u_y = -\frac{\partial \psi}{\partial x}. \tag{4}$$

All quantities are dimensionless. Parameters appearing in the problem are the Reynolds, Grashof and Prandtl numbers, defined as

$$Re = Ud/\nu, \quad Gr = g\beta(T_1 - T_0)\, d^3/\nu^2, \quad Pr = \nu/\kappa, \tag{5}$$

where ν = kinematic viscosity, κ = thermal diffusivity, β = volume thermal expansion coefficient and g = acceleration of gravity (directed downward). All properties are constant except for density in the buoyancy term (the Boussinesq approximation).

The problem is cast in time-dependent form for convenience in the numerical computation. Initial conditions are arbitrary and were typically taken to be a fluid at rest. Boundary conditions are those appropriate to impermeable no-slip walls ($u_x = u_y = 0$, except at the moving wall, where $u_x = 1$).

Equations (1) to (4) with appropriate boundary conditions are solved by an explicit time marching technique. Forward time and central space differences are used except for the convection terms in (1) and (2) for which a special three-point non-central difference is employed. Details of the technique are provided by Torrance & Rockett (1969). The calculation proceeds by advancing T and ω

with difference forms of (1) and (2). Equation (3) is solved by the method of successive over-relaxation for the new ψ field, which is then used to obtain the velocities (from difference forms of (4)) and the wall vorticity (which requires the velocity boundary conditions). Stability of the scheme follows by restricting the time step; no restrictions are imposed on the spatial mesh. All fields are current and the calculation can proceed with a further time advancement.

3. Results

This investigation covers a range of Grashof numbers, $Gr = 0, \pm 10^4, \pm 10^6$, and a range of cavity aspect ratios, $h/d = \frac{1}{2}, 1, 2$. A Prandtl number typical of gases was assumed, $Pr = 1$, and the Reynolds number was held fixed at $Re = 100$.

The numerical solution procedure yielded the entire flow transient. The final flows were always steady and the same final flow was obtained using different initial data. Since the transients were always smooth transitions from one field to another there is no need to present them here. Instead, only the final steady-state flows will be considered. Those interested in the transients are referred to Donovan (1970).

3.1. *Steady-state streamline and temperature fields*

Computed flow and temperature fields are illustrated in figures 1–3. Streamlines and isotherms were obtained by interpolation between grid points and the ψ and T values are indicated. The outer boundary corresponds to $\psi = 0$, the moving wall to $T = 1$, and the stationary walls to $T = 0$. The locations of interior maxima or minima of the ψ field are shown by crosses in all figures. Negative and positive ψ values correspond to clockwise and counter-clockwise circulation respectively.

Figure 1 illustrates the effect of buoyancy on the flow in cavities of three different aspect ratios. Figure 1 (*a*) corresponds to $Gr = 10^4$, figure 1 (*b*) to $Gr = 0$ and figure 1 (*c*) to $Gr = -10^4$. The algebraic sign of Gr is determined by the product $g\beta(T_1 - T_0)$. With gravity directed downward and β positive (true for most fluids) the case $Gr > 0$ corresponds to a hot upper wall and the case $Gr < 0$ to a cold upper wall. For $Re = 100$ and $|Gr| = 10^4$, the coefficient $GrRe^{-2}$ of the buoyancy term in the vorticity equation (2) is of unit order. The contribution of buoyancy to the vorticity is therefore $O(1)$. The contribution of wall shear to vorticity is found from detailed analysis of the case $Gr = 0$ to be $O(10)$ near the moving wall and significantly less in the lower parts of the cavities, especially those of larger aspect ratios. It is in the bottom of the larger aspect ratio cavities that wall shear and buoyancy effects become of the same magnitude (see figure 1), as indicated by the stronger influence of buoyancy on the flows.

Results for $Gr = 0$ (figure 1 (*b*)) are included primarily for comparison purposes. A single primary eddy exists for $h/d = \frac{1}{2}$ and 1, and a secondary eddy appears for $h/d = 2$. Small corner eddies appear for all cases. Results given by Burggraf (1966) for a square cavity using a fine mesh are virtually coincident with those given here, as measured by the magnitude of the circulation, location of the vortex centre, and the appearance and shape of the streamlines (including

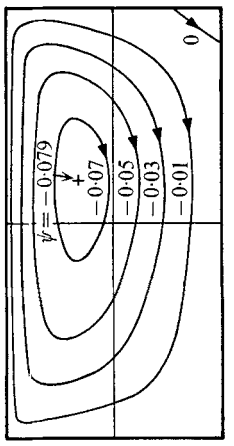

FIGURE 1(*c*) (i)

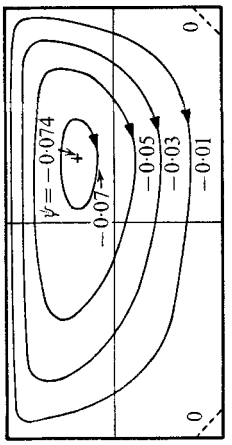

FIGURE 1(*b*) (i)

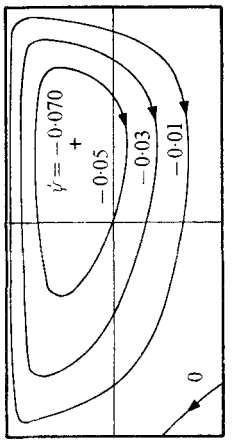

FIGURE 1(*a*) (i)

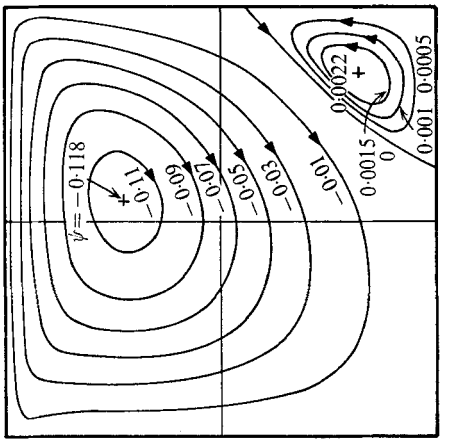

FIGURE 1(*c*) (ii)

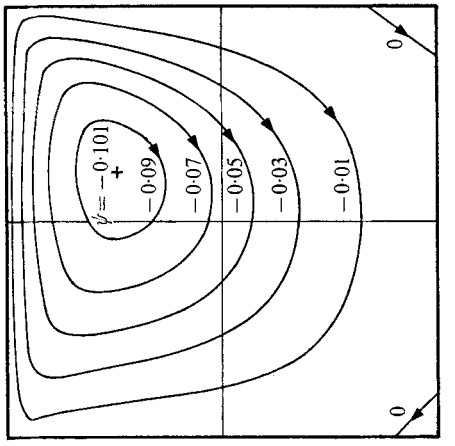

FIGURE 1(*b*) (ii)

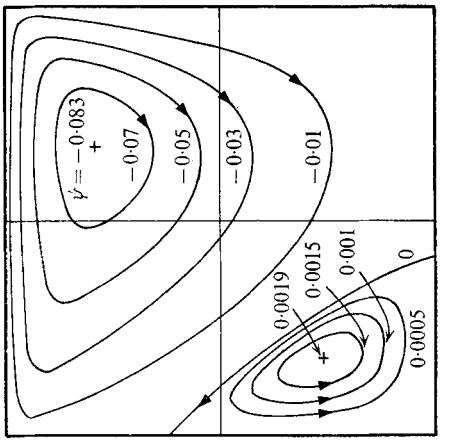

FIGURE 1(*a*) (ii)

FIGURE 1(*a–c*) (i–ii). For legends see facing page.

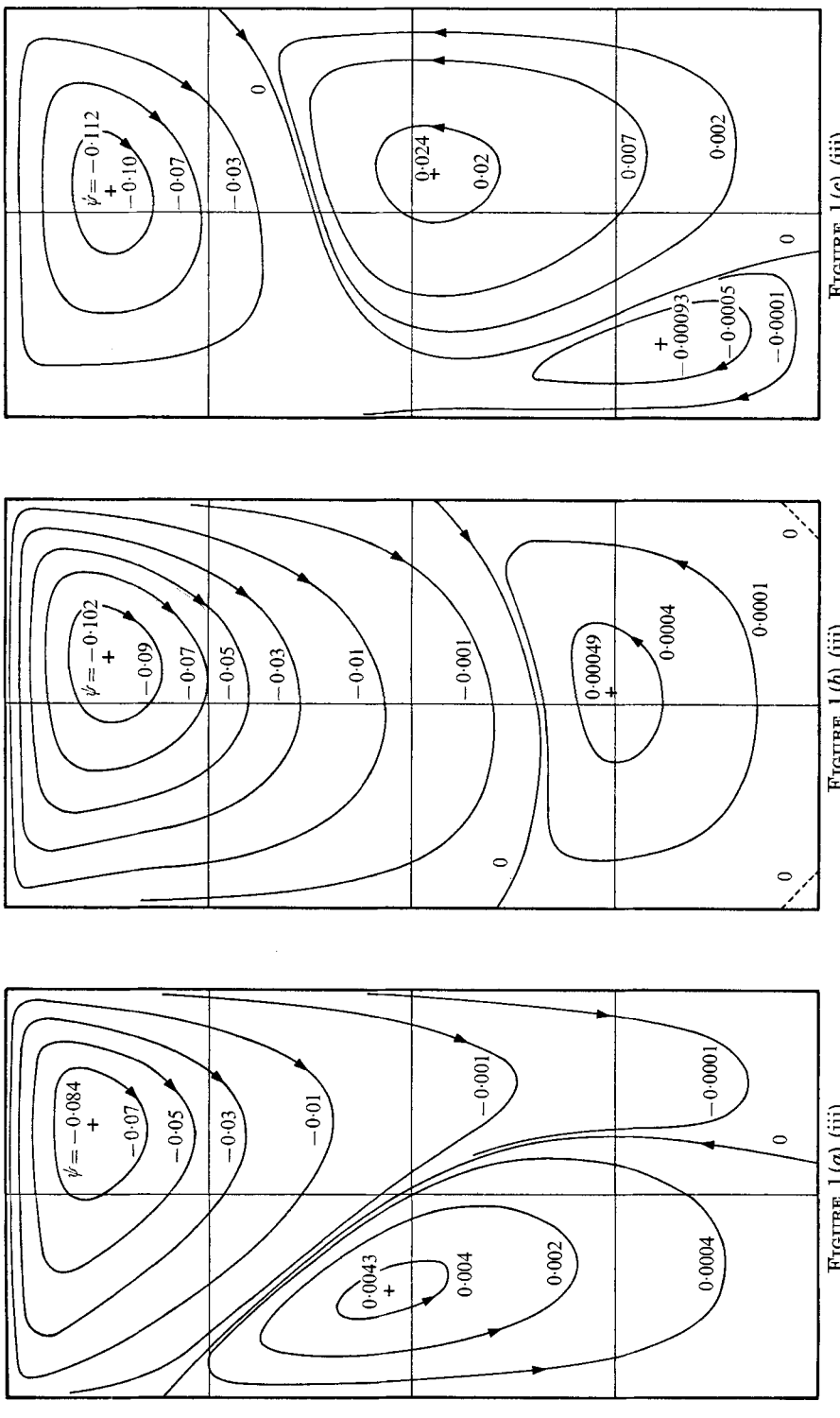

FIGURE 1 (*a*) (iii) FIGURE 1 (*b*) (iii) FIGURE 1 (*c*) (iii)

FIGURE 1. Steady-state streamline fields for $Re = 100$ and $Pr = 1$. (*a*) $Gr = 10^4$, aspect ratio $h/d = \frac{1}{2}$, 1, 2 for (i), (ii), (iii) respectively. (*b*) $Gr = 0$, $h/d = \frac{1}{2}$, 1, 2 for (i), (ii), (iii) respectively. (*c*) $Gr = -10^4$, $h/d = \frac{1}{2}$, 1, 2 for (i), (ii), (iii) respectively.

corner eddies). Burggraf concluded that a fine mesh is required to achieve quantitative results. As noted in the next section, however, the present numerical method yields significantly better results for a given mesh spacing than does Burggraf's method.

The mesh increments used here ($\Delta x = \Delta y = 0{\cdot}05$ for $h/d = 1$ and 2, $\Delta x = 0{\cdot}05$, $\Delta y = 0{\cdot}025$ for $h/d = \frac{1}{2}$) are believed to yield quantitative information. Velocity profiles and streamlines for $h/d = \frac{1}{2}$ and 1 from this study are in very close agreement with the work of Donovan (1970) and in fair agreement with the work of Mills (1965) and Kawaguti (1961), who used comparatively coarser mesh spacings.

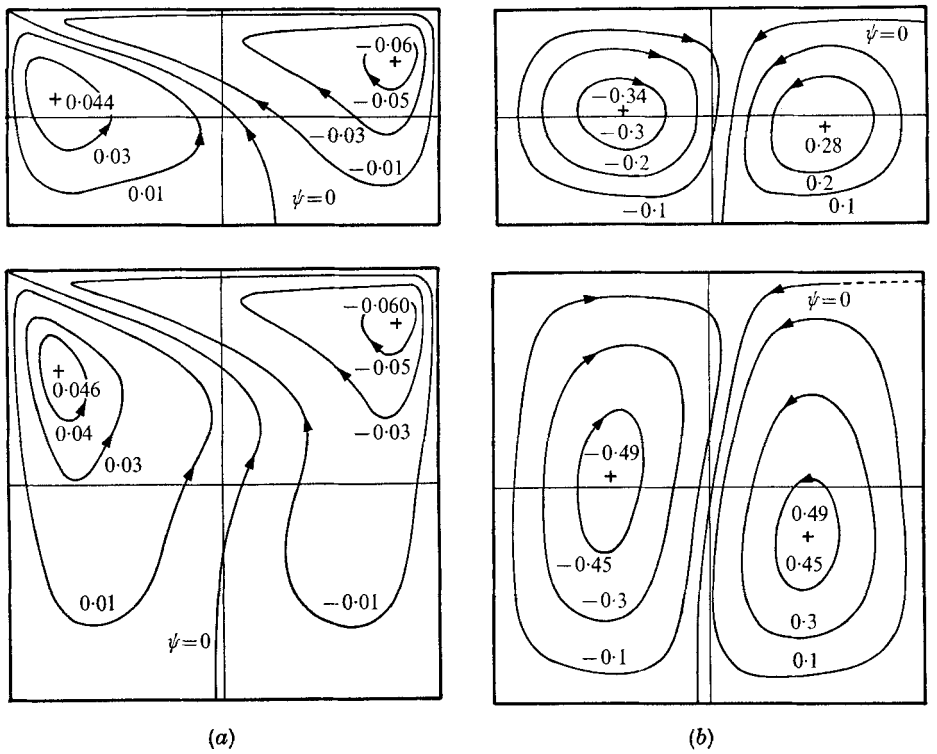

FIGURE 2. Steady-state streamline fields for cavities with $Re = 100$ and $Pr = 1$. (*a*) $Gr = 10^6$, (*b*) $Gr = -10^6$, $h/d = \frac{1}{2}$, 1 for the upper and lower pairs of figures respectively.

The effect of a heated upper wall, $Gr = 10^4$ (figure 1 (*a*)), is to enhance the left corner eddy and to diminish both the right corner eddy (which is no longer discernible) and the strength of the primary eddy. Warm buoyant fluid tends to remain near the top. A cooled upper wall, $Gr = -10^4$ (figure 1 (*c*)), has the reverse effect. The primary circulation increases as cold fluid is accelerated toward the bottom, and the right corner eddy grows as the cooler interior fluid is accelerated vertically near the warmer walls. For the tall cavity a local minimum in the stream function develops near the bottom.

Figure 2 presents streamlines for $Gr = \pm 10^6$ for $h/d = \frac{1}{2}$ and 1. Circulation is decreased below that shown in figure 1 for $Gr = 10^6$, whereas the reverse is true

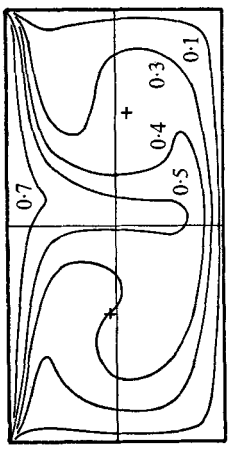

FIGURE 3 (*c*) (i)

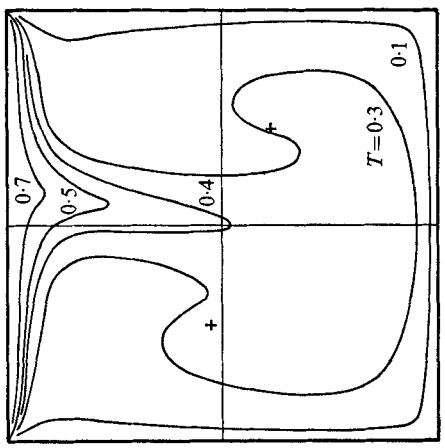

FIGURE 3 (*c*) (ii)

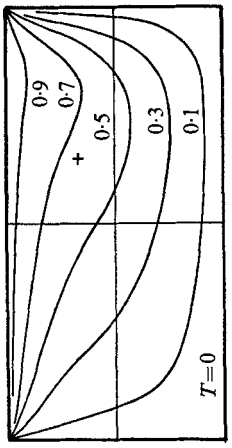

FIGURE 3 (*b*) (i)

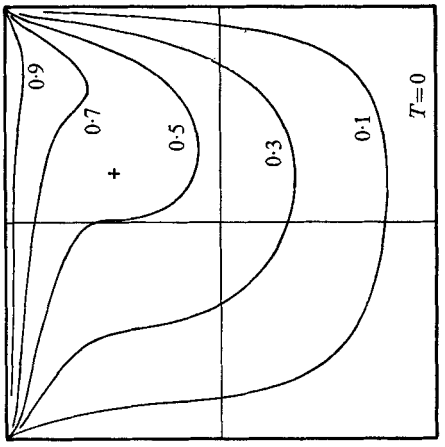

FIGURE 3 (*b*) (ii)

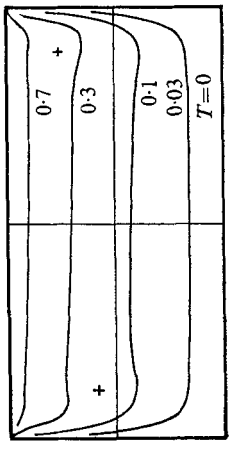

FIGURE 3 (*a*) (i)

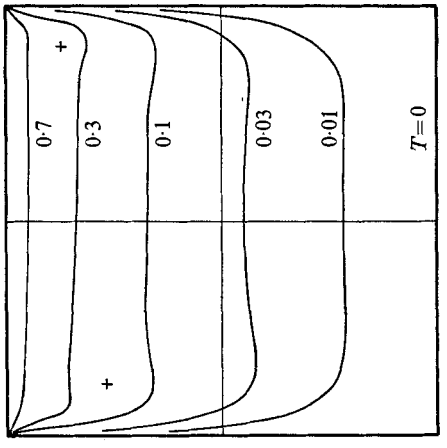

FIGURE 3 (*a*) (ii)

FIGURE 3 (*a–c*) (i–ii). For legend see p. 228.

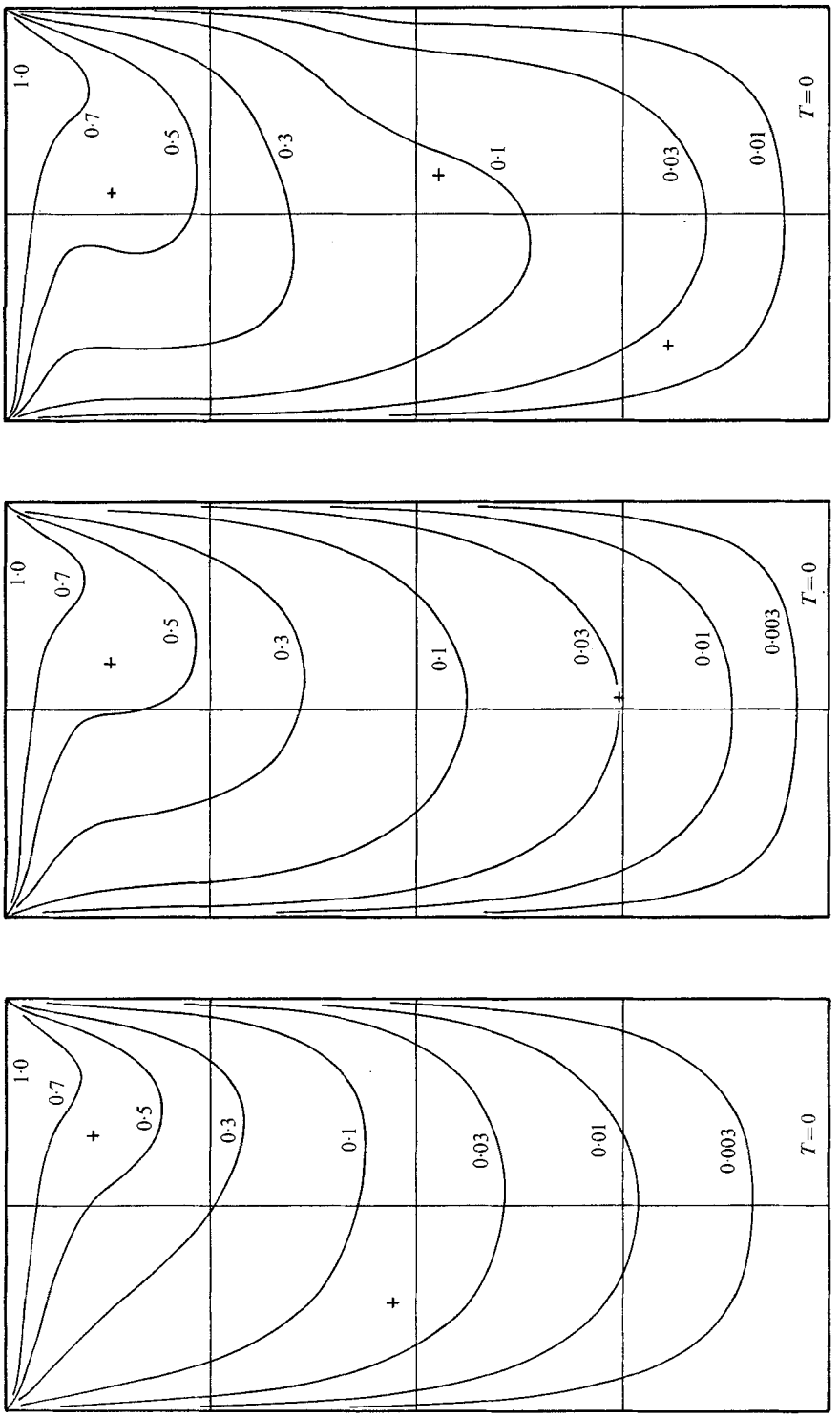

FIGURE 3 (a) (iii) FIGURE 3 (b) (iii) FIGURE 3 (c) (iii)

FIGURE 3. Steady-state temperature fields for cavities with $Re = 100$ and $Pr = 1$. (a) $Gr = 10^6$, $h/d = \frac{1}{2}$, 1 for (i), (ii) respectively; $Gr = 10^4$, $h/d = 2$ for (iii). (b) $Gr = 0$, $h/d = \frac{1}{2}$, 1, 2 for (i), (ii), (iii) respectively. (c) $Gr = -10^6$, $h/d = \frac{1}{2}$, 1 for (i), (ii) respectively; $Gr = -10^4$, $h/d = 2$ for (iii).

for $Gr = -10^6$. In each case shown in figure 2 two approximately equal eddies develop. For a pure buoyancy flow without a moving wall, two symmetric eddies would be expected; it thus appears that buoyancy effects dominate the flows. The streamlines near the top are distorted to accommodate the moving wall. The influence of buoyancy at $|Gr| = 10^6$ is to be expected, of course, since the coefficient $Gr\,Re^{-2}$ of the buoyancy term is of $O(100)$.

Temperature fields are shown in figure 3. Results in figure 3(*b*) ($Gr = 0$) and figures 3(*a*, iii), 3(*c*, iii) ($h/d = 2$) correspond to the streamline fields given in figure 1. The remaining temperature fields (figures 3(*a*; i, ii), (*b*; i, ii) for $h/d = \frac{1}{2}$ and 1) correspond to the streamline fields at $Gr = \pm 10^6$ given in figure 2. This method of presentation is employed to conserve space, since the temperature fields for all cavities at $Gr = 0, \pm 10^4$ were very similar. This is apparent from inspection of results for $h/d = 2$, which show the largest variation of the isotherms with Gr of all the cavities. A given isotherm moves towards the top for $Gr = 10^4$ and towards the bottom for $Gr = -10^4$ as the fluid circulation is retarded or enhanced respectively. Although the temperature fields are remarkably similar the corresponding streamlines are not.

Temperature fields for $h/d = \frac{1}{2}$ and 1 show a striking variation for $Gr = 0, \pm 10^6$ which correlates closely with the corresponding flow patterns. For $Gr = 10^6$, temperature stratification is apparent, whereas for $Gr = -10^6$, buoyancy is effective in stimulating circulation. The temperature field in the square cavity at $Gr = 0$ may be compared with similar results of Burggraf (1966). There is a very slight difference in isotherms near the top of the cavity for the two methods. This may be due, in part, to the failure of Burggraf's method to satisfy energy conservation. This is discussed in the next section.

3.2. *Convergence of the numerical method*

A number of mesh sizes (Δx, Δy) were employed and it is possible to check the convergence of the numerical results. Such a check is presented in figure 4, which displays the minimum value of stream function within the mesh versus $(\Delta x)^2$. For all cases $\Delta x = \Delta y$. The figure pertains to the case $Re = 100$, $Pr = 1$ and $Gr = 0$, but results are similar for other values of Gr. Results from the present study are shown with open circles and open squares for aspect ratios of one and two respectively. Data of Burggraf (1966) for an aspect ratio of one are shown by crosses.

In the method of presentation used in figure 4, results for a numerical method which is correct to second order (i.e. $O(\Delta x)^2$) should be described by a straight line. A linear relation is apparent for Burggraf's method and the present method, at least at small mesh increments. For larger mesh increments some deviation is expected and is observed. This is due in part to the fact that the quantities being compared did not occur at precisely the same spatial location for all grids. Note that all results tend toward the same limit as $(\Delta x)^2$ tends to zero.

The observed trend of Burggraf's data is not surprising because his method is formally correct to second order. What is surprising, however, is that the present method appears to be correct to the same order. This method employs a special formulation of the convection terms which has a formal accuracy of $O(\Delta x)$. The

failure of this truncation error to dominate is only partially explained by the generally smaller velocities that exist away from the moving wall.

Another feature of note in figure 4 is the rate of convergence of the present method as compared to Burggraf's method. Clearly the present method is closer to the exact solution at all values of $(\Delta x)^2$. Indeed, a mesh increment of $\Delta x = 0{\cdot}05$ yields results comparable to a mesh with $\Delta x = 0{\cdot}028$ using Burggraf's method.

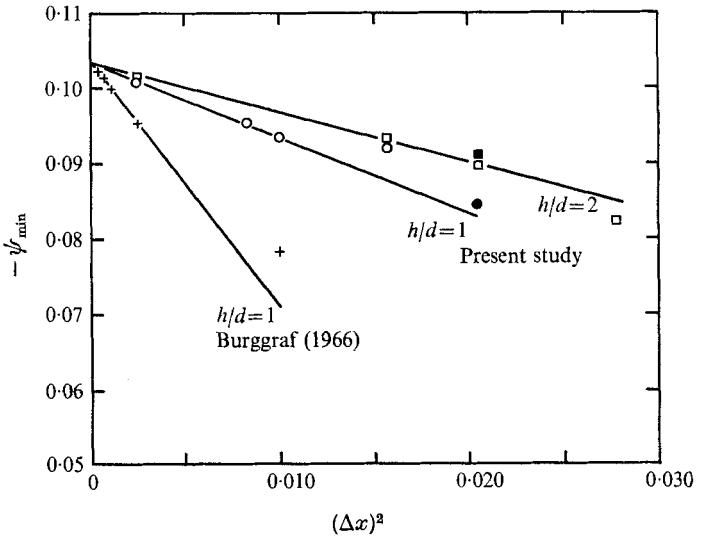

FIGURE 4. Minimum value of stream function in the cavity for various mesh spacings: +, $h/d = 1$, Burggraf (1966); ○, $h/d = 1$, present study; ●, $h/d = 1$, method of Fromm (1964); □, $h/d = 2$, present study; ■, $h/d = 2$, method of Fromm (1964). Comparison presented for the case $Re = 100$, $Pr = 1$, $Gr = 0$.

From Burggraf's data, a mesh of the latter size can be expected to yield quantitative information. Some related observations on the convergence of methods is presented in Gosman *et al.* (1969).

The principle reason for the apparently better results obtained with the present method is the use of the conservation form of the convection terms in equations (1) and (2). A finite-difference representation of these terms leads to conservation of energy and vorticity within the grid system. Use of the alternate forms $\mathbf{u}.\nabla T$ and $\mathbf{u}.\nabla\omega$ (obtained by using the equation of continuity) leads to difference representations which do not conserve energy and vorticity within the grid system. Implications of conservation are discussed more fully by Torrance & Rockett (1969). For comparison, two additional data points obtained by using a second-order correct method that conserves energy and vorticity in the convection terms (see Fromm 1964) are shown as a filled circle and a filled square for $h/d = 1$ and 2 respectively. Clearly, the second-order conserving method is significantly better than the second-order non-conserving form and is (apparently) comparable to or slightly better than the present method. Numerical stability for Fromm's method appears to involve a restriction on mesh size which may not always be met, for practical reasons.

The authors wish to gratefully thank Cornell University for providing necessary time on an IBM 360/65 computer.

REFERENCES

BATCHELOR, G. K. 1956 *J. Fluid Mech.* **1**, 177.

BURGGRAF, O. R. 1966 *J. Fluid Mech.* **24**, 113.

DONOVAN, L. F. 1970 *N.A.S.A. Tech. Memo.* X-52767.

FROMM, J. 1964 In *Methods in Computational Physics*, vol. 3, p. 345. Academic.

GOSMAN, A. D., PUN, W. M., RUNCHAL, A. K., SPALDING, D. B. & WOLFSHTEIN, M. 1969 *Heat and Mass Transfer in Recirculating Flows*, pp. 159–167. Academic.

GREENSPAN, D. 1969 *Computer J.* **12**, 88.

KAWAGUTI, M. 1961 *J. Phys. Soc. Japan*, **16**, 2307.

MILLS, R. D. 1965 *J. Roy. Aero. Soc.* **69**, 714.

NEWELL, M. E. & SCHMIDT, F. W. 1970 *J. Heat Transfer, Trans. A.S.M.E.* C **92**, 159.

PAN, F. & ACRIVOS, A. 1967 *J. Fluid Mech.* **28**, 643.

SIMUNI, L. M. 1964 *Inzhenernii Zhournal*, **4**, 446.

SQUIRE, H. B. 1956 *J. Roy. Aero. Soc.* **60**, 203.

TORRANCE, K. E. & ROCKETT, J. A. 1969 *J. Fluid Mech.* **36**, 33.

WEISS, R. F. & FLORSHEIM, B. H. 1965 *Phys. Fluids*, **8**, 1631.